Journal of Materials Chemistry A

Cationic polymer binders inhibit shuttle effects through electrostatic confinement for lithium sulfur batteries

Journal:	*Journal of Materials Chemistry A*
Manuscript ID	TA-ART-11-2017-010239.R2
Article Type:	Paper
Date Submitted by the Author:	19-Mar-2018

Complete List of Authors:	Wang, Huali; Beijing Institute of Technology Ling, Min; Zhejiang university Bai, Ying; Beijing Institute of Technology, School of Chemical Engineering and the Environment Chen, Shi; Beijing Institute of Technology, School of Chemical Engineering and the Environment Yuan, Yanxia; Beijing Institute of Technology, Liu, G; Laurence Berkley National Laboratory, Environmental Energy Technologies Division Wu, Chuan; Beijing Institute of Technology, School of Chemical Engineering and the Environment Wu, Feng; Beijing Institute of Technology, School of Chemical Engineering and the Environment

SCHOLARONE™
Manuscripts

Cationic polymer binders inhibit shuttle effects through electrostatic confinement for lithium sulfur batteries

Huali Wang[a,b,1], Min Ling[b,c,1], Ying Bai[a,*], Shi Chen[a,d], Yanxia Yuan[a], Gao Liu[b,*], Chuan Wu[a,d*], Feng Wu[a,d]

Received 00th January 20xx,
Accepted 00th January 20xx

DOI: 10.1039/x0xx00000x

www.rsc.org/

Irreversible chemical reactions always cause capacity fade and poor cycle life of Lithium-Sulfur (Li-S) batteries due to irreversible lithium polysulfides. An unexpected cationic polymer strategy at the Lawrence Berkeley National Lab shows a capture of irreversible polysulfides, which does greatly enhance the Li-S cycling performance. The branched polyethylenimine (PEI) polymer with a high density amine group can trap the lithium polysulfide through the interaction between -NH in amine group and soluble Li_2S_x. To boost the interaction, cationization is achieved through nucleophilic substitution with CH_3I; the cationic PEI (denoted as MPEII) has enhanced affinity to polysulfides. It attracts not only the lithium polysulfide through Li-N and Li-I attraction, but also the S_x^{2-} by electrostatic attraction of positively charged N after cationization. The cell with MPEII binder shows a better performance than PEI in self-discharge test. It also achieved a high S loading of 6.5 mg/cm^2, with a high areal capacity of 6.48mAh/cm^2 and a corresponding 985mAh/g after10 cycles.

Introduction

The increasing large-scale grid and electric vehicles demand call for high density and low cost energy storage devices. Lithium sulfur batteries well satisfied all requirements due to its high specific capacity (1675mAh/g) and energy density of 2600 Wh/kg, which are five times higher than those of conventional lithium-ion batteries based on intercalation compound cathodes.[1-5] Moreover, sulfur is rich in nature resources, extremely low cost, light weight and environmental friendliness.[6-11] Different from lithium-oxygen/air battery, which is another high-energy battery system, the Li-S battery is a closed system, avoiding exposure to atmospheric contamination and potential safety hazards.[12] Despite these advantages, the realization of sulfur batteries has been hindered by a few inherent drawbacks. First, the low electrical conductivities of both sulfur and sulfides limit electron transport in the electrode and lead to low utilization of active material.[13, 14] Second, the dissolving lithiated products result in shuttle effect that sulfur species transport between electrodes, conducing to low Coulombic efficiency and active material loss.[15,16] In addition, the volume change of Li anode and cathode during cycling gives rise to serious side reactions between the soluble lithiated intermediate and lithium metal, which leads to fast capacity fade and related to safety issues.[17-20] To address these issues, most efforts have been focused in carbon matrix confinement.[21] Such as porous carbon,[22-24] carbon nanotubes[25-29] and conductive polymers[30] have been utilized to enhance the utilization of active sulfur. It came out that the physically trapped polysulfide will eventually leach into the electrolyte again after few cycles. Thus, chemical immobilization, e.g., surface-functionalized carbon,[31,32] metal oxide/sulfide materials[33,34] and especially binder modification[35-39] turns out to be a promising solution.[40]

The binder acts as an indispensable component in battery, contributing to bonding and keeping the active materials, which enhancing electrical contact between the active materials and conductive carbon, as well as current collector.[14, 41] Therefore, a perfectible binder have a significantly effect on battery performance.[42-48] The functional groups in binders are investigated to immobilize the soluble lithium polysulfide through either C-S bond, N-Li bond or O-Li bond,[10] i.e., polyvinylpyrrolidone (PVP),[49] polyamidoamine (PAMAM) dendrimers,[36] PAN,[50] PFM,[35] and gum Arabic,[51] Polyethylenimine (PEI) polymer, bearing a large amount of amine groups in each molecular unit. The amino groups of PEI are chemically reactive and consequently enable a wide variety of chemical modifications which provide PEI with appropriate physicochemical properties.[52,53] Researchers in Lawrence Berkeley National Lab have already revealed the effective electrostatic confinement of polysulfides in lithium/sulfur batteries by a PEI.[54] To boost the interaction, here we propose an enhanced affinity to polysulfides through the stronger electrostatic force of PEI derived polymers. The cationic PEI is designed to confine lithium polysulfides through interacting with the both Li^+ and S^{2-}_x ions. Analysis of the interaction is simulated through the theoretical calculation method with density functional theory (DFT) prior the electrochemical test.

Material and methods

Theoretical calculation

Gaussian 09 software,[55] with Density Functional Theory (DFT) method at the B3LYP/6-311++G(d, p) theory level was used to optimize conformations and calculate the adsorption energies. Mixed basis were used for I contained molecule, in which 6-311++G(d, p) basis was used for C, N, H, Li, S atoms, while LANL2DZ basis was used for I atom. A few initial configurations were tested in each case to obtain qualitative trends, and small variations were expected depending on the initial configuration thus giving rise to different local minima. GaussView was used to process the data and generate electrostatic potential (ESP) maps. Each ESP map used consistent isovalues and color scaling for related compounds. The adsorption energies of Li_2S_6 on the

[a] Beijing Key Laboratory of Environmental Science and Engineering, School of Materials Science & Engineering, Beijing Institute of Technology, No. 5 South Zhongguancun Street, Beijing 100081, China. E-mail: membrane@bit.edu.cn (Y. Bai), chuanwu@bit.edu.cn (C. Wu)
[b] Applied Energy Material groups, Energy Storage and Distributed Resources Division, Lawrence Berkeley National Laboratory, Berkeley, CA 94720, USA
[c] Key Laboratory of Biomass Chemical Engineering of Ministry of Education, College of Chemical and Biological Engineering, Zhejiang University, Hangzhou 310027, China. E-mail: gliu@lbl.gov (Gao Liu)
[d] Collaborative Innovation Center of Electric Vehicles in Beijing, Beijing 100081, China

†Electronic Supplementary Information (ESI) available: See DOI: 10.1039/x0xx00000x

substrates are defined by△Eads=-[E(Sub-Li_2S_6)-E(Sub)-E(Li_2S_6)] where E(Sub), E(Li_2S_6) and E(Sub-Li_2S_6) stand for the calculated electronic energies of the bare substrates, Li_2S_6 and the anchoring systems, respectively.[40] Here, the higher values of ΔEads indicates the stronger anchoring interaction and vice versa.

Synthesis and Characterization

The micrometric sulfur powder is purchased form Sigma-Aldrich, Super C45 is purchased from TIMCAL, and Graphene is purchased from XG Sciences. All the other chemicals in this work were purchased from Sigma-Aldrich and used without further purification except specifically notified. PEI cationic polymer was synthesized by reaction of PEI and CH_3I at the mole ratio of 4:1 (CH_3I to monomer units of PEI). 5g PEI (Mw25000) was dissolved in 20 ml 1,4-Dioxane, then 6g CH_3I was added with stirring for 1h at room temperature. The white precipitate was collected and dried in a vacuum oven at 50℃ for 24h. FTIR characterization of synthesized cationic polymer was collected on a Mattson Galaxy 300 spectrometer.

Cathode fabrication

All cathode slurries were prepared in aqueous solvents. Sulfur powder, Super C45 and Graphene are added into the binder solution according to a certain weight ratio. The mixture is mixed by a ball-milling method for 48 hours to obtain homogeneous slurry. Then the slurry was coated onto an aluminum current collector with a doctor blade using an Elcometer motorized film applicator. The coated slurry was allowed to air-dry for 4 hours. Finally, 1.26 cm^2 cathodes were punched out and dried in a vacuum oven for 12 hours at 50℃ before their transfer into an argon-filled glove box for coin cell assembly. The typical mass loading of sulfur is 6.5 mg/cm^2. The composition of cathode is S:C45:Graphene:binder=50:30:10:10 (weight ratio).

Cell assembly and testing

Coin cells (CR2325, National Research Council Canada) were assembled in an argon-filled glove box with O_2 and H_2O content less than 0.5 ppm. Lithium metal foil was used as anode and polypropylene celgard 2400 was used as separator. The electrolyte was 1M lithium bis(trifluoromethanesulfonyl)imide (LiTFSI) dissolved in a mixture of 1,3-dioxolane and dimethoxyethane(1:1 in volume) with 2% $LiNiO_3$ added as an additive to help passive the surface of the lithium anode and reduce the shuttle effect. The electrochemical performance was measured galvanostatically in a voltage range of 1.8-2.6V on a Maccor series 4000 cell tester at 30℃. The self-discharge test was performed at 0.05C rate (1C=1672 mA/g), by charging the cells to the fully charged state and then letting them rest for 60 hours. This procedure was repeated three times, with the third rest lasting 240 hours. The charge/discharge specific capacities were calculated based on the mass of S in the electrodes. Cells used for SEM characterization were tested at 0.05C for 5 cycles, and stopped at fully charged or fully discharged state. Then these cells were disassembled in argon-filled glove box, finally the cathodes were washed thoroughly using DME/DOL(1:1) solvent and dried before SEM study.

Results and discussion

Theoretical investigation on interactions of Li_2S_6 with cationic polymer binder

PEI is a potential cationic polymer due to the abundant amine groups in each monomer. The cationization is achieved through methylation with CH_3I. I^- is one of the best leaving groups, which could facilitate the Coulomb interaction between the positively charged amine group and S_x^{2-}. To simulate the confine mechanism, theoretical calculation method was adopted to give a systematical understanding toward the polysulfides anchoring effects. Li_2S_6 is integrated in the simulation since its high solubility in electrolyte.[55] Considering branched PEI is a large polyamine structure composed of primary, secondary, and tertiary amines, we choose a representative structure containing these three kinds of amine group for simplification. Methyl iodide was chosen as the methylation reagent. The partially methylated PEI iodide is noted as MPEII in the following text. Nucleophilic substitution occurred

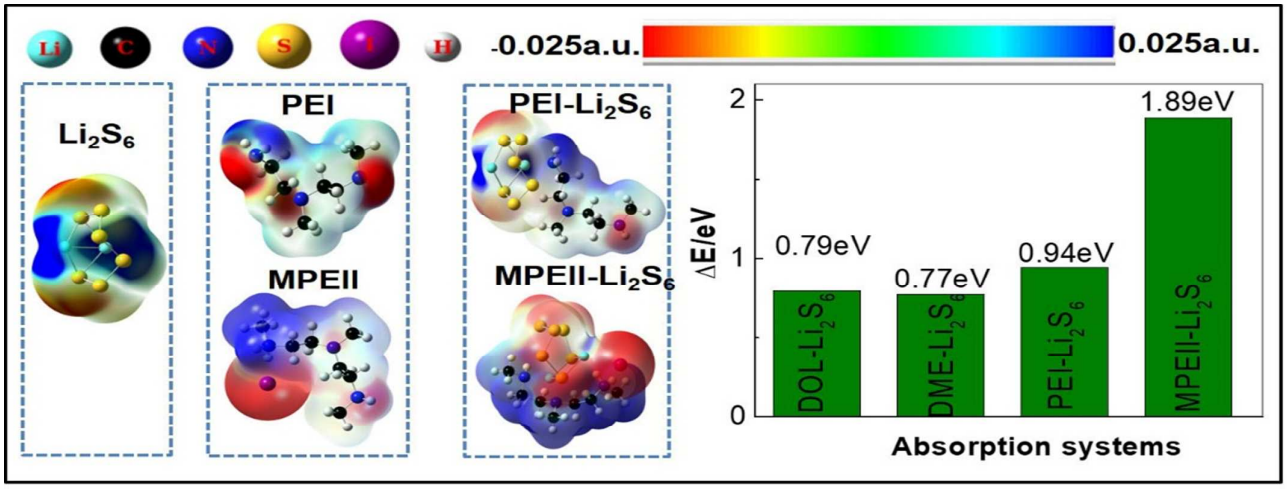

scheme 1 Polysulfide confine mechanism and calculated binding energy of adsorption systems. ESP maps of Li_2S_6, PEI, MPEII, PEI-Li_2S_6 and MPEII-Li_2S_6 are shown. All maps used consistent surface potential ranges (−0.025 au (red) to 0.025 au (blue)) and an isovalue of 0.001 a.u.

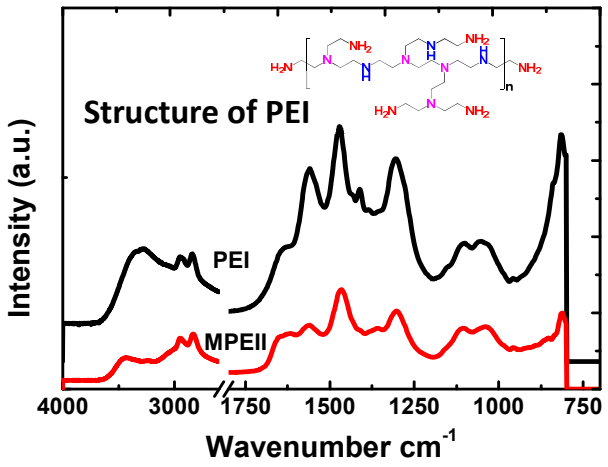

Figure 1 IR-ATR spectra of PEI and MPEII.

preferentially with primary amine, then the secondary amines and finally tertiary amines. The simulation is mainly focused on primary amine group to evaluate the bondage intensity.

As shown in Scheme 1, molecules are displayed with the optimized ground state structure and electrostatic potential (ESP) maps. Based on the ESP maps, possible sites of interaction could be predicted through the charge distribution. The more redish the color in the maps, the higher the electron density. It can be found that the optimized Li_2S_6 exhibits a ring-like configuration with the two Li^+ ions located on the opposite sides of the ring.[40] Although the primary, secondary, and tertiary amine groups own different electron density in PEI, all of them exhibit strong electronegativity which attracts the Li ions and thus anchors the S_6^{2-} anions.

To achieve the electrostatic absorption strategy, amine groups are methylated by methyl iodide (CH_3I) first to become cationic. The N atom is positively charged after cationization. The methylated amine groups will directly connected to the negatively charged S_6^{2-} anions after the leaving of I^-.[56] After the nucleophilic substitution of CH_3I, the charge distribution of MPEII is simulated as shown in scheme 1.

The adsorption strength between binders and lithium polysulfides should be prevail to the dissolution into the electrolyte solvents. Hence, the adsorption energy is also quantified through simulation. The calculated adsorption energies of Li_2S_6 on different molecule are shown in Scheme 1. The adsorption energy for DOL-Li_2S_6 and DME-Li_2S_6 is 0.79eV and 0.77eV, respectively. In contrast, the binding energy of PEI-Li_2S_6 anchoring system is 0.94eV, which is higher than that of DOL-Li_2S_6 and DME-Li_2S_6. For MPEII, the binding energy is 1.89eV, which is the highest among the interactions.

Synthesis and characterize of MPEII cationic polymer

The designed MPEII was synthesized by reaction of CH_3I with the branched PEI at the mole ratio of 4:1 (CH_3I to monomer units of PEI). The IR-ATR spectra of production are shown in Figure 1, insertion is the structure formula of PEI unit. Characteristic peaks of PEI at 3270 cm^{-1} (–N–H stretching), 2940–2830 cm^{-1} (–C–H stretching), 1558 cm^{-1} (–N–H bending), 1473 cm^{-1} (–C–H bending) and 1350–1000 cm^{-1} (–C–N stretching) can be found in the MPEII. The peak of stretching vibration of –N–H appeared at 3270 cm^{-1} in the spectrum of PEI transfers to 3440 cm^{-1} in the spectrum of MPEII, with an intensity decrease. Peaks at 2929 and 2839 cm^{-1} attributed to the C-H vibration on CH_2 also have a blue-shift in MPEII.

Electrolyte Uptake of the polymer binders

Due to the coating of binders on the bulk sulfur material, lithium ion diffusion in the polymer binder is critical for the cycling performance of L-S battery, because of the binder. In our system, the lithium ion diffusion in polymer binders is measured through

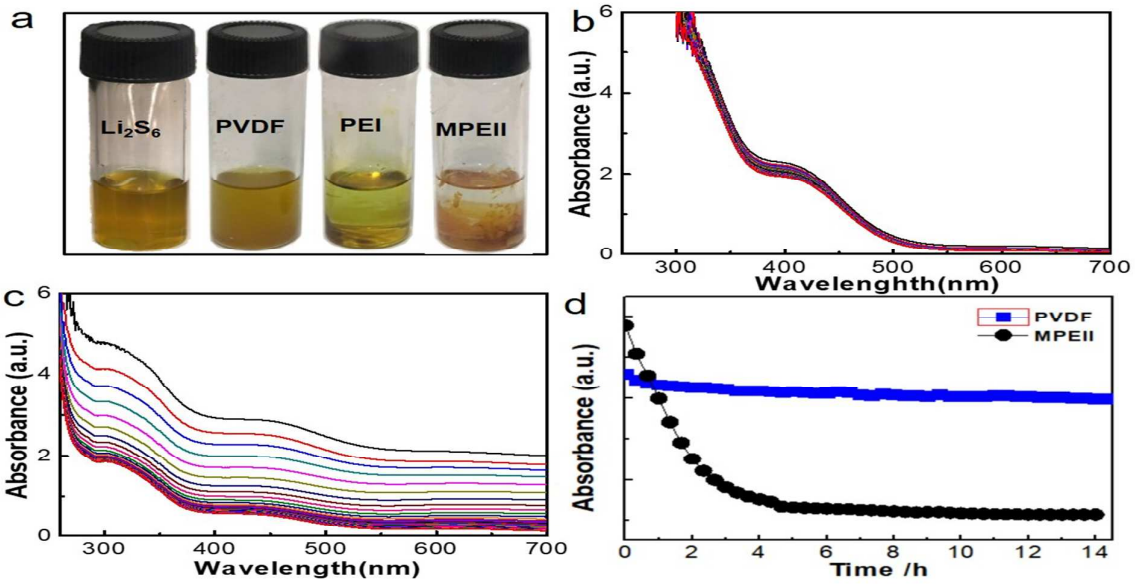

Figure 2 (a) Photo images of lithium polysulfide (Li_2S_6) solution before and after addition of binders; (b,c) The time-lapsed UV–vis absorbance of the in situ UV–vis spectra of PVDF and MPEII binder in 3 mmol/L polysulfide dissolved in DOL/DME solution; (c) The absorbance change of the in situ UV–vis absorbance as a function of time for PVDF and MPEII polymer.

electrolyte uptake. As shown in Figure S1, the total electrolyte uptake is around 10-11% of its final weight after 7 days for both PEI and MPEII. The iodide ions play a limited role in the polarity.

In situ UV-vis investigation on interactions of Li_2S_6 with cationic polymer binder

Besides the theoretical calculation, the adsorption abilities of PVDF, PEI and MPEII on lithium polysulfides were examined. The experimental phenomena of polysulfide solutions after adding these binders are shown in Figure 2a. It can be seen that after adding binder for 48h, solution with both PEI and MPEII binder show much lighter color compared to the pristine, while no change is found in solution with PVDF. The color of solution indicates the adsorption ability of polysulfides. MPEII shows the best adsorption ability since the color is almost disappeared.

In-situ ultraviolet-visible spectroscopy (UV-vis) is conducted to confirm the electrostatic confinement as shown in Figure 2(b-d). The 0.1g polymers are soaked in the 1-mL 3-mmol/L long-chain lithium polysulfide (average formula Li_2S_6) in 1M Bis(trifluoromethane)sulfonimide lithium salt (LiTFSI) in 1,3-dioxolane (DOL)/ 1,2-dimethoxyethane (DME) electrolyte for 14 hours to track the polysulfide concentration evolution. The *in situ* spectra indicate that Li_2S_6 species produce characteristic peaks in around 430 nm. A significant polysulfide concentration decrease is recorded for the solution exposed to MPEII polymer. In contrast, the absorption signals for polysulfide solution exposed to PVDF hold constant, indicating limited interaction of PVDF with polysulfide over 14 hours.

Galvanostatic lithiation/delithiation performance

The cycling performances are all based on high loading electrodes, which are composed of 50 wt% micro-size sulfur particles. As shown in Figure 3a, a high initial capacity of 6.23 mAh/cm^2 was reached for PEI based electrode, corresponding to a sulfur utilization of 61.8% with the sulfur loading of 5.98 mg/cm^2. The specific capacity is stable at ca. 500 mAh/g for both PEI and MPEII based electrode as presented in Figure S2. Self-discharge tests were conducted to study the polysulfides absorption ability of PEI and MPEII binder in Li-S batteries as shown in Figure 3a. The rest procedures are set after the 10th, 20th, and 30th cycles at a fully charged status. The corresponding rest time is 60 h, 60 h and 240 h, respectively. The self-discharge prevention ability of cathode is characterized by three factors: (1) The self-discharge prevention factor, which shows the capability to prevent capacity loss during the rest; (2) The reversible capacity retention factor, which shows the ratio of capacity could be recovered after rest; (3) Open circuit voltage drop, which shows the polysulfide dissolution during the rest. The self-discharge prevention factor shown in Figure 3b was calculated by formula $Q_p=C_a/C_b$, C_a is the discharge capacity after rest, and C_b is the discharge capacity before rest. The reversible capacity retention factor shown in Figure 3c was calculated by formula $Q_r=C_f/C_b$, C_f is the discharge capacity of the following cycle after rest. The Q_p and Q_r trends in Figure 3b and c indicate that MPEII shows better self-discharge prevention ability and reversible capacity retention than PEI. The loss of lithium polysulfides could also be illustrated through the variation of open circuit voltage during rest in Figure 3d. MPEII exhibits a much slower voltage drop compared to PEI.

The cationization of PEI obviously alleviates the shuttle effect through the electrostatic interaction with the negatively charged polysulfide anions. Hence, a higher content of MPEII are investigated as shown in Figure 4. The result confirmed that the self-discharge prevention ability and reversible capacity retention are improved with the increasing binder content up to 20 wt%. However, it comes out that the electrode with 15% binder shows the highest areal capacity of 7.13 mAh/cm^2 in Figure 4a. It could be ascribed to the compromise between the increasing absorption capability and decreasing conductivity. The areal capacity is stable at ca. 4.0 mAh/cm^2 in the following cycles, corresponding to a specific capacity of ca. 670 mAh/g as shown in Figure S3. The Q_p and Q_r trends in Figure 4b and c indicate that S cathode with 20 wt% MPEII shows the best self-discharge prevention ability and

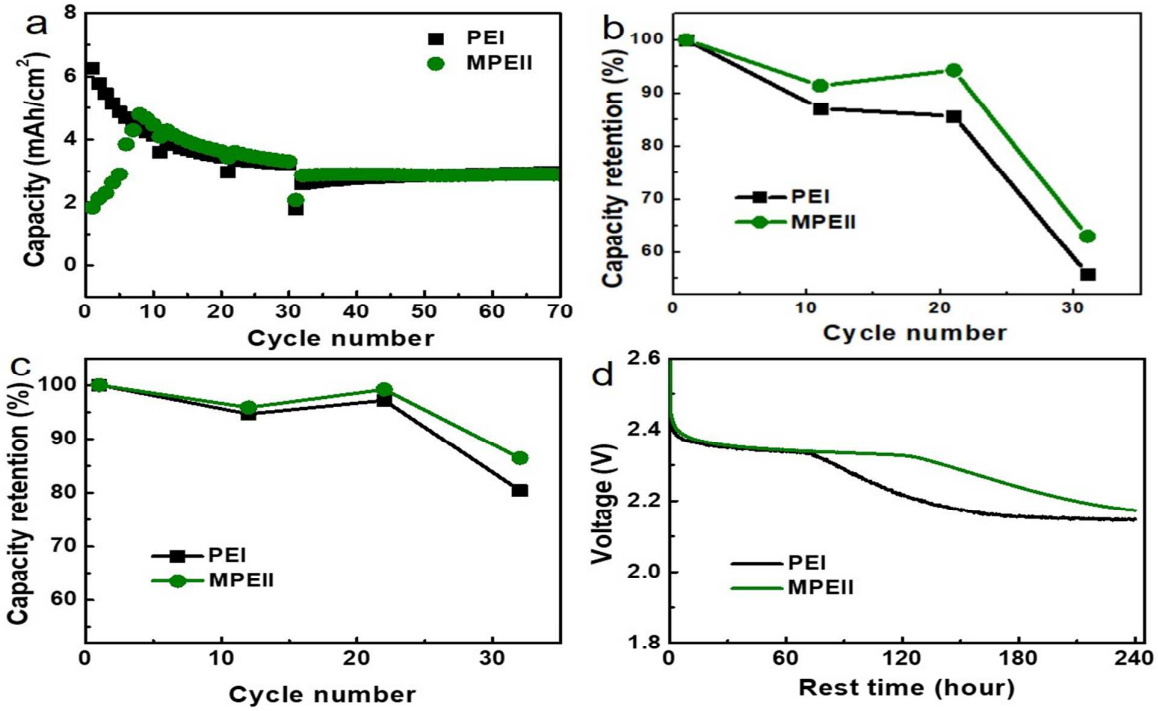

Figure 3 (a) Cycling performance of PEI and MPEII based sulfur electrodes at 0.05C; (b) Capacity retention ratio of cycle immediate after rest(Q_p); (c) Capacity retention ratio of the following cycle after rest(Q_r); (d) Open circuit voltage change versus rest time for the 240 hour self-discharge rest.

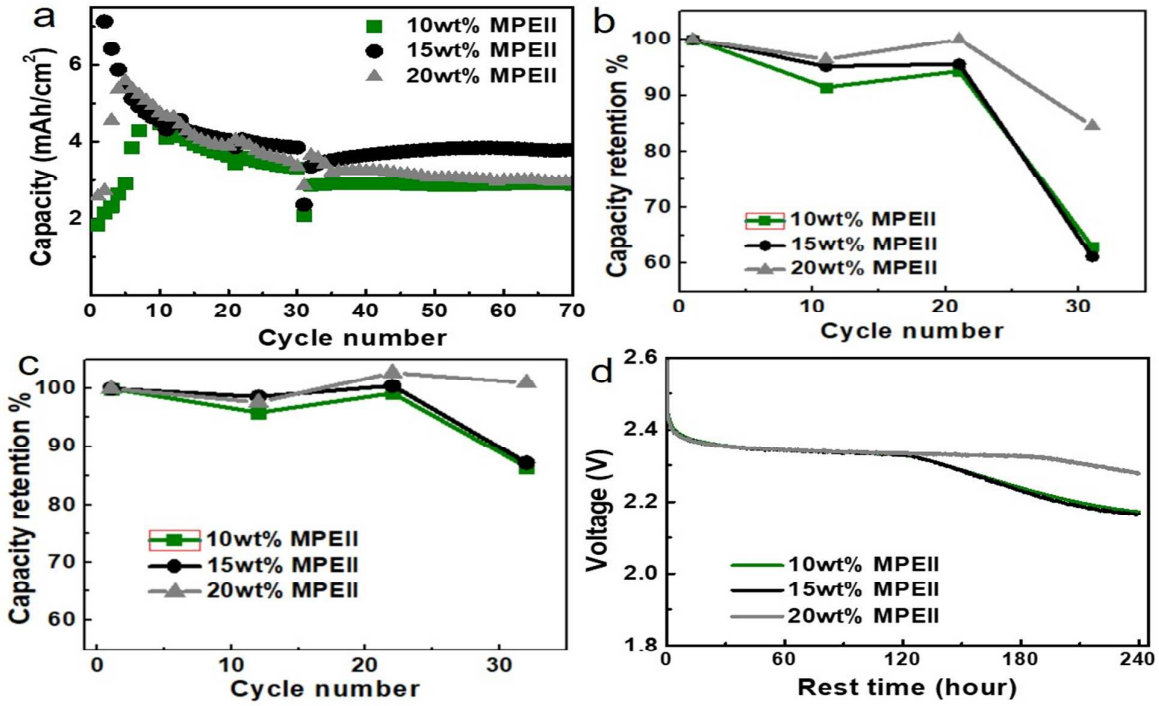

Figure 4 (a) Cycling performance of cathodes with vary MPEII binder content; (b) Capacity retention ratio of cycle immediate after rest (Q_p); (c) Capacity retention ratio of the following cycle after rest (Q_r); (d) Open circuit voltage change vs. rest time during the third self-discharge rest.

reversible capacity retention. A much slower voltage drop is found during rest, as shown in Figure 4d, which also indicates that a higher MPEII content resulted in enhanced affinity to polysulfides.

Based on the optimized binder proportion, the rate performance of MPEII based electrodes were investigated as shown in Figure S4. All cells for rate performance test were cycled with a sulfur loading of ca. 6.30 mg/cm^2 between 1.8–2.6 V. For such a high loading, high areal capacity of 7.52 mAh/cm^2 (1160 mAh/g) is still obtained as show in Figure S4a and S3b. The capacity is stabilized at 5 mAh/cm^2 (ca. 710 mAh/g) on cycling at 0.05C. When the current density increased to 0.1 C, the cycling capacity could be stable at ca. 4 mAh/cm^2. A relatively high capacity of 3 mAh/cm^2 is still obtained at 0.3C. The specific capacity profiles for all rates performance is presented in Figure S4c. Considering cells capacity stabilized after 10 cycles, the galvanostatical charge/discharge profiles at the 10th cycle are shown in Figure S4c. The typical two discharge plateaus at 2.3V and 2.0V are observed at 0.05C. An increasing polarization is found with the increasing rate. Afterwards, the long term cycle performance is recorded at 1C based on the 15 wt% MPEII polymer binder as shown in Figure S5. The capacity fade fast due to the high mass loading of around 6.0 mg.

Morphology of cathodes with different binders in lithiated and delithiated state

To investigate the morphology evolution after lithiatino/delithiation, SEM images of sulfur are shown in Figure 5. All fresh prepared cathodes show a uniform sulfur, carbon and iodine distribution, which can also be verified in the Energy Dispersive Spectra (EDS) mapping in Figure S6 and S7. In fully lithiated state, porosity was found to be decreased after the deposition of the lithiated product, i.e., Li_2S. For PEI, the solid-phase Li_2S precipitations congregate on the surface of cathode, as shown in Figure 5b. While for MPEII, Li_2S precipitation is uniformly distributed in cathode matrix. Fully delithiated cathodes (Figure 5c and 5f) show the similar morphology to fresh prepared cathodes, which means a good reversibility was achieved on each cathode. The long chain sulfur species were trapped in cathode matrix without much dissolution. This trend is accord with electrochemical performance of cathode.

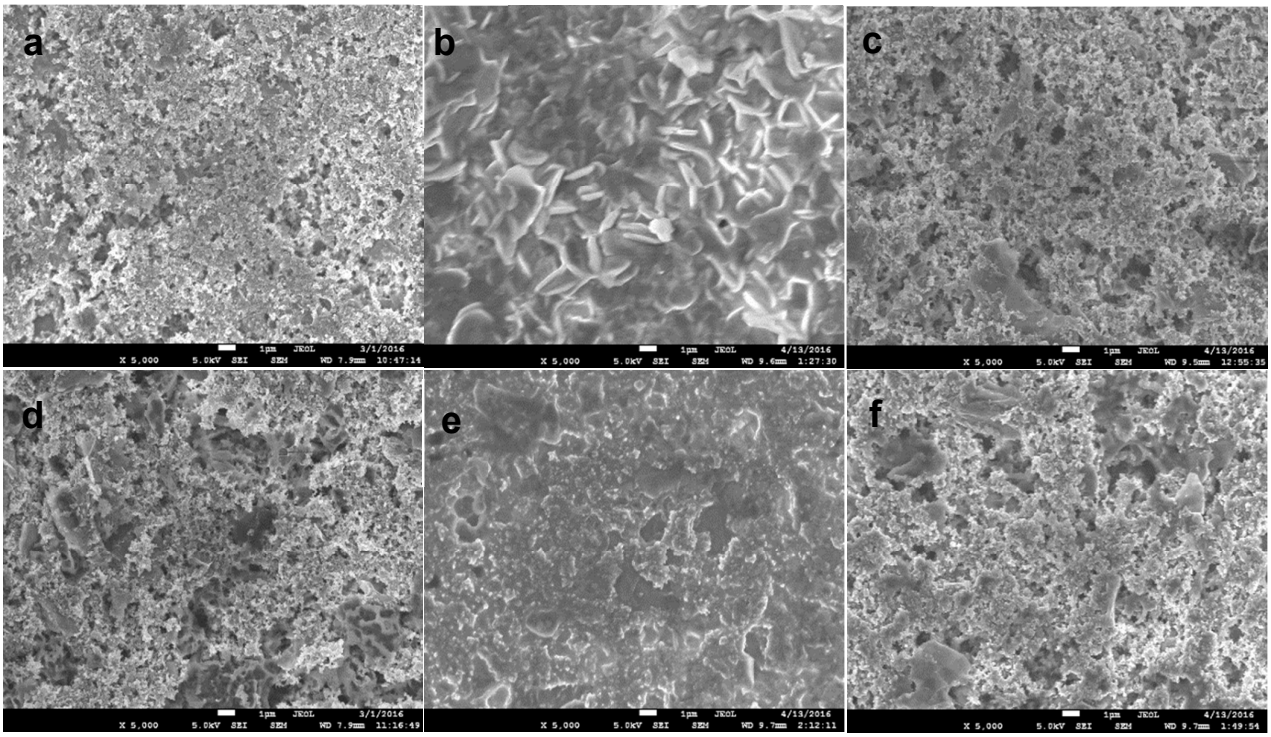

Figure 5 SEM images of PEI (a-c) and MPEII (d-f) based pristine (left), lithiated (middle) and delitihated (right) sulfur electrodes with 5,000× magnification.

Conclusions

A cationic polymer binder was designed and superior performance of S cathode with this binder was obtained. Both the experimental and calculation results show that the nitrilerich and positive charge contained MPEII binder have a higher binding affinity to polysulfides than PEI. It indicates that electrostatic attraction could become an effective way in polysufur confining. By physically and chemically trapped the polar lithium polysulfides, S cathode with MPEII binder shows rather good self-discharge performance. A high areal capacity of 6.48mAh/cm^2 and a high specific capacity of 985mAh/g at 10th cycle are achieved, with high S loading of 6.5 mg/cm^2, when the discharge rate is 0.05C.

Acknowledgement

This work was supported by the National Basic Research Program of China (Grant No. 2015CB251100). Lawrence Berkeley National Laboratory was supported by the U.S. Department of Energy, Office of Science, Office of Basic Energy Sciences, under Contract No. DE-AC02-05CH11231.

Notes and references

1 Y. V. Mikhaylik and J. R. Akridge, *J. Electrochem. Soc.*, 2003, **150**, A306-A311.
2 Y. K. Sun, S. T. Myung, B. C. Park, J. Prakash, I. Belharouak and K. Amine, *Nat. Mater.*, 2009, **8**, 320-324.
3 P. Strubel, S. Thieme, T. Biemelt, A. Helmer, M. Oschatz, J. Brückner, H. Althues and S. Kaskel, *Adv. Funct. Mater.*, 2015, **25**, 287-297.
4 B. Scrosati, J. Hassoun and Y. K. Sun, *A look into the future*, 2011, 4, 3287-3295.
5 T. Lei, W. Chen, J. Huang, C. Yan, H. Sun, C. Wang, W. Zhang, Y. Li and J. Xiong, *Adv. Energy Mater.*, 2017, **7**, 1601843.
6 M. Armand and J. M. Tarascon, *Nature*, 2008, **451**, 652-657.
7 P. G. Bruce, *Solid State Ionics*, 2008, **179**, 752-760.
8 B. Dunn, H. Kamath and J. M. Tarascon, *Science*, 2011, **334**, 928-935.
9 Y. Yang, G. Zheng and Y. Cui, *Chem. Soc. Rev.*, 2013, **42**, 3018-3032.
10 A. Manthiram, Y. Fu, S. H. Chung, C. Zu and Y. S. Su, *Chem. Rev.*, 2014, **114**, 11751-11787.
11 L. X. Miao, W. K. Wang, A. B. Wang, K. G. Yuan and Y. S. Yang, *J. Mater. Chem*. A, 2013, 1, 11659-11664.
12 H. Peng, J. Huang, X. Cheng and Q. Zhang, *Adv. Energy Mater.*, 2017, 1700260.
13 Q. Zhao, X. Hu, K. Zhang, N. Zhang, Y. Hu and J. Chen, *Nano Lett.*, 2015, **15**, 721-726.
14 W. Chen, T. Qian, J. Xiong, N. Xu, X. Liu, J. Liu, J. Zhou, X. Shen, T. Yang, Y. Chen and C. Yan, *Adv. Mater.*, 2017, **29**, 1605160.
15 S. H. Chung, P. Han, R. Singhal, V. Kalra and A. Manthiram, *Adv. Energy Mater.*, 2015, **5**, 1500738.
16 Y. S. Su, Y. Fu, T. Cochell and A. Manthiram, *Nature Commun.*, 2013, **4**, 2985.

17 X. B. Li, P. Guo, T. F. Cao, H. Liu, W. M. Lau and L. M. Liu, *Scientific Reports*, 2015, **5**, 10848.
18 X. B. Cheng, R. Zhang, C. Z. Zhao, F. Wei, J. G. Zhang and Q. Zhang, *Adv. Sci.*, 2016, **3**, 1500213.
19 N. W. Li, Y. X. Yin, C. P. Yang and Y. G. Guo, *Adv. Mater.*, 2016, **28**, 1853-1858.
20 R. Zhang, X. Cheng, C. Zhao, H. Peng, J. Shi, J. Huang, J. Wang, F. Wei and Q. Zhang, *Adv. Mater*., 2016, **28**, 2155-2162.
21 X. Jiantie, S. Jianglan, W. Jianli, W. Min, L. Hua-Kun, D. Shi Xue, J. In-Yup, S. Jeong-Min, B. Jong-Beom and D. Liming, *ACS Nano*, 2014, **8**, 10920-10930.
22 W. Zhang, D. Qiao, J. Pan, Y. Cao, H. Yang and X. Ai, *Electrochem. Acta*, 2013, **87**, 497-502.
23 Z. Li, Y. Jiang, L. Yuan, Z. Yi, C. Wu, Y. Liu, P. Strasser and Y. Huang, *Acs Nano*, 2014, **8**, 9295-9303.
24 Y. Zhong, X. H. Xia, S. J. Deng, J. Y. Zhan, R. Y. Fang, Y. Xia, X. L. Wang, Q. Zhang and J. P. Tu, *Adv. Energy Mater.* 2018, **8**,
25 L. Liu, S. H. Chung and A. Manthiram, *J. Mater. Chem. A*, 2016, **4**, 16805-16811.
26 B. Duan, W. Wang, A. Wang, K. Yuan, Z. Yu, H. Zhao, J. Qiu and Y. Yang, *J. Mater. Chem. A*, 2013, 1, 13261-13267.
27 J. Ye, F. He, J. Nie, Y. Cao, H. X. Yang and X. Ai, *J. Mater. Chem. A*, 2015, **3**, 7406-7412.
28 L. Zhu, W. C. Zhu, X. B. Cheng, J. Q. Huang, H. J. Peng, S. H. Yang and Q. Zhang, *Carbon,* 2014, **75**, 161-168.
29 H. J. Peng, W. T. Xu, L. Zhu, D. W. Wang, J. Q. Huang, X. B. Cheng, Z. Yuan, F. Wei and Q. Zhang, *Adv. Funct. Mater.*, 2016, **26**, 6351-6358.
30 L. Yan, D. Han, M. Xiao, S. Ren, Y. Li, S. Wang and Y. Meng, *J. Mater. Chem. A*, 2017, **5**, 7015-7025.
31 L. Ma, H. L. Zhuang, S. Wei, K. E. Hendrickson, M. S. Kim, G. Cohn, R. G. Hennig and L. A. Archer, *ACS Nano*, 2016, **10**, 1050-1059.
32 T. Z. Hou, H. J. Peng, J. Q. Huang, Q. Zhang and B. Li, *2D Mater.*, 2015, **2**, 014011.
33 Q. Pang, D. Kundu and L. F. Nazar, *Materials Horizons*, 2016, **3**, 130-136.
34 Z. Yuan, H. J. Peng, T. Z. Hou, J. Q. Huang, C. M. Chen, D. W. Wang, X. B. Cheng, F. Wei and Q. Zhang, *Nano Lett*., 2016, **16**, 519-527.
35 G. Ai, Y. Dai, Y. Ye, W. Mao, Z. Wang, H. Zhao, Y. Chen, J. Zhu, Y. Fu and V. Battaglia, *Nano Energy*, 2015, **16**, 28-37.
36 P. Bhattacharya, M. I. Nandasiri, D. Lv, A. M. Schwarz, J. T. Darsell, W. A. Henderson, D. A. Tomalia, J. Liu, J. G. Zhang and J. Xiao, *Nano Energy*, 2015, **19**, 176-186.
37 Q. Pang, X. Liang, C. Y. Kwok, J. Kulisch and L. F. Nazar, *Adv. Energy Mater.*, 2017, **7**, 1601630.
38 X. L. Jia and L. F. Nazar, *J. Mater. Chem.*, 2010, **20**, 9821-9826.
39 Z. W. Seh, H. T. Wang, P. C. Hsu, Q. F. Zhang, W. Y. Li, G. Y. Zheng, H. B. Yao and Y. Cui, *Energy Environ. Sci.*, 2014, **7**, 672-676.
40 Z. Ji, B. Han, Q. Li, C. Zhou, Q. Gao, K. Xia and J. Wu, *J. Phys. Chem. C,* 2015, **119**, 20495-20502.
41 G. Li, M. Ling, Y. Ye, Z. Li, J. Guo, Y. Yao, J. Zhu, Z. Lin and S. Zhang, *Adv. Energy Mater.*, 2015, **5**, 1500878.
42 L. Min, J. Qiu, L. Sheng, Y. Cheng, M. J. Kiefel, L. Gao and S. Zhang, *Nano Lett*., 2015, **15**, 4440-4447.
43 M. J. Lacey, F. Jeschull, K. Edström and D. Brandell, *Chem. Commun.,* 2013, **49**, 8531-8533.
44 A. Shyamsunder, W. Beichel, P. Klose, Q. Pang, H. Scherer, A. Hoffmann, G. K. Murphy, I. Krossing and L. F. Nazar, *Angew. Chem.*, 2017, **56**, 6192-6197.
45 J. Liu, H. Nara, T. Yokoshima, T. Momma and T. Osaka, *J. Power Sources,* 2015, **273**, 1136-1141.
46 Y. C. Tsao, Z. Chen, S. Rondeau-Gagné, Q. F. Zhang, H. B. Yao, S. C. Chen, G. M. Zhou, C. X. Zu, Y. Cui and Z. N. Bao, *ACS Energy Lett.* 2017, **2**, 2454-2462.
47 W. Y. Li, Q. F. Zhang, G. Y. Zheng, Z. W. Seh, H. B. Yao and Y. Cui, *Nano Lett.* 2013, **13**, 5534-5540.
48 P. Bhattacharya, M. I. Nandasiri, D. P. Lv, A. M. Schwarz, J. T. Darsell, W. A. Henderson, D. A. Tomalia, J. Liu, J. G. Zhang and J. Xiao, *Nano Energy*, 2016, **19**, 176-186.
49 M. J. Lacey, F. Jeschull, K. Edström and D. Brandell, *J. Power Sources*, 2014, **264**, 8-14.
50 S. Wei, L. Ma, K. E. Hendrickson, Z. Tu and L. A. Archer, *J. Am. Chem. Soc.,* 2015, **137**, 12143-12152.
51 G. Li, M. Ling, Y. Ye, Z. Li, J. Guo, Y. Yao, J. Zhu, Z. Lin and S. Zhang, *Adv. Energy Mater*., 2015, **5**, 1500878.
52 I. Yudovin-Farber, J. Golenser, N. Beyth, E. I. Weiss and A. J. Domb, *J. Nanomater.*, 2010, **2010**, 139-143.
53 Y. Jung and S. Kim, *Electrochem. Commun.*, 2007, **9**, 249-254.
54 L. Zhang, M. Ling, J. Feng, G. Liu and J. Guo, *Nano Energy*, 2017, **40**, 559-565.
55 M. J. Frisch, G. W. Trucks, H. B. Schlegel, G. E. Scuseria, M. A. Robb, J. R. Cheeseman, G. Scalmani, V. Barone, B. Mennucci, G. A. Petersson, H. Nakatsuji, M. Caricato, X. Li, H. P. Hratchian, A. F. Izmaylov, J. Bloino, G. Zheng, J. L. Sonnenberg, M. Hada, M. Ehara, K. Toyota, R. Fukuda, J. Hasegawa, M. Ishida, T. Nakajima, Y. Honda, O. Kitao, H. Nakai, T. Vreven, J. A. Montgomery Jr., J. E. Peralta, F. Ogliaro, M. J. Bearpark, J. Heyd, E. N. Brothers, K. N. Kudin, V. N. Staroverov, R. Kobayashi, J. Normand, K. Raghavachari, A. P. Rendell, J. C. Burant, S. S. Iyengar, J. Tomasi, M. Cossi, N. Rega, N. J. Millam, M. Klene, J. E. Knox, J. B. Cross, V. Bakken, C. Adamo, J. Jaramillo, R. Gomperts, R. E. Stratmann, O. Yazyev, A. J. Austin, R. Cammi, C. Pomelli, J. W. Ochterski, R. L. Martin, K. Morokuma, V. G. Zakrzewski, G. A. Voth, P. Salvador, J. J. Dannenberg, S. Dapprich, A. D. Daniels, Ö. Farkas, J. B. Foresman, J. V. Ortiz, J. Cioslowski and D. J. Fox, Gaussian, Inc., Wallingford, CT, USA. 2009.
56 E. P. Kamphaus and P. B. Balbuena, *J. Phys. Chem. C*, 2016. **120**, 4296-4305.